



Swansea University
Prifysgol Abertawe



Cronfa - Swansea University Open Access Repository

This is an author produced version of a paper published in:

Physical Biology

Cronfa URL for this paper:

<http://cronfa.swan.ac.uk/Record/cronfa43257>

Paper:

Jing, X., Loskot, P. & Yu, J. (2018). How does supercoiling regulation on a battery of RNA polymerases impact on bacterial transcription bursting?. *Physical Biology*

<http://dx.doi.org/10.1088/1478-3975/aad933>

This item is brought to you by Swansea University. Any person downloading material is agreeing to abide by the terms of the repository licence. Copies of full text items may be used or reproduced in any format or medium, without prior permission for personal research or study, educational or non-commercial purposes only. The copyright for any work remains with the original author unless otherwise specified. The full-text must not be sold in any format or medium without the formal permission of the copyright holder.

Permission for multiple reproductions should be obtained from the original author.

Authors are personally responsible for adhering to copyright and publisher restrictions when uploading content to the repository.

<http://www.swansea.ac.uk/library/researchsupport/ris-support/>

ACCEPTED MANUSCRIPT

How does supercoiling regulation on a battery of RNA polymerases impact on bacterial transcription bursting?

To cite this article before publication: Xiaobo Jing *et al* 2018 *Phys. Biol.* in press <https://doi.org/10.1088/1478-3975/aad933>

Manuscript version: Accepted Manuscript

Accepted Manuscript is “the version of the article accepted for publication including all changes made as a result of the peer review process, and which may also include the addition to the article by IOP Publishing of a header, an article ID, a cover sheet and/or an ‘Accepted Manuscript’ watermark, but excluding any other editing, typesetting or other changes made by IOP Publishing and/or its licensors”

This Accepted Manuscript is © 2018 IOP Publishing Ltd.

During the embargo period (the 12 month period from the publication of the Version of Record of this article), the Accepted Manuscript is fully protected by copyright and cannot be reused or reposted elsewhere.

As the Version of Record of this article is going to be / has been published on a subscription basis, this Accepted Manuscript is available for reuse under a CC BY-NC-ND 3.0 licence after the 12 month embargo period.

After the embargo period, everyone is permitted to use copy and redistribute this article for non-commercial purposes only, provided that they adhere to all the terms of the licence <https://creativecommons.org/licenses/by-nc-nd/3.0>

Although reasonable endeavours have been taken to obtain all necessary permissions from third parties to include their copyrighted content within this article, their full citation and copyright line may not be present in this Accepted Manuscript version. Before using any content from this article, please refer to the Version of Record on IOPscience once published for full citation and copyright details, as permissions will likely be required. All third party content is fully copyright protected, unless specifically stated otherwise in the figure caption in the Version of Record.

View the [article online](#) for updates and enhancements.

How does supercoiling regulation on a battery of RNA polymerases impact on bacterial transcription bursting?

Xiaobo Jing¹ Pavel Loskot^{1,2} Jin Yu^{1*}

1.Beijing Computational Science Research Center, 100193, P.R. China

2.Systems and Process Engineering Centre, Swansea University, SA28PP, U.K

Email: jinyu@csrc.ac.cn

Abstract

Transcription plays an essential role in gene expression. The transcription bursting in bacteria has been suggested to be regulated by positive supercoiling accumulation in front of a transcribing RNA polymerase (RNAP) together with gyrase binding on DNA to release the supercoiling. In this work, we study the supercoiling regulation in the case of a battery of RNAPs working together on DNA by constructing a multi-state quantitative model, which allows gradual and stepwise supercoiling accumulation and release in the RNAP transcription. We solved for transcription characteristics under the multi-state bursting model for a single RNAP transcription, and then simulated for a battery of RNAPs on DNA with T7 and *E. coli* RNAP types of traffic, respectively, probing both the average and fluctuation impacts of the supercoiling regulation. Our studies show that due to the supercoiling accumulation and release, the number of RNAP molecules loaded onto the DNA vary significantly along time in the traffic condition. Though multiple RNAPs in transcription promote the mRNA production, they also enhance the supercoiling accumulation to suppress the production. In particular, the fluctuations of the mRNA transcripts become highly pronounced for a battery of RNAPs transcribing together under the supercoiling regulation, especially for a long process of transcription elongation. In such an elongation process, though a single RNAP can work at a high duty ratio, multiple RNAPs are hardly able to do so. Our multi-state model thus provides a systematical characterization of the quantitative features of the bacterial transcription bursting; it also supports improved physical examinations on top of this general modeling framework.

Keywords: transcription burst, DNA supercoiling, RNA Polymerase (RNAP)

Introduction

Transcription is the first key step of gene expression. It is directed by RNA polymerases (RNAPs), the protein enzymes that move along double-stranded (ds) DNA and catalyze polymerization chain reactions to synthesize messenger RNA (mRNA) based on DNA template [1, 2]. The complete transcription includes initiation, elongation, and termination. A transcription bubble forms during the initiation, in which the RNAP enzyme starts unwinding dsDNA downstream. The unwound DNA strands reanneal afterwards upstream to the transcribing RNAP. It had been recognized in a twin-supercoiled-domain model that in front of and behind an elongating RNAP, positive and negative DNA supercoiling build up [3-5], respectively, as the dsDNA under transcription is subject to topological constraints at two ends to be prevented from freely rotating. Notably, it has been found in bacterial transcription systems, when the negative supercoiling can be quickly resolved by sufficiently abundant topoisomerase I (Topo I), the positive supercoiling built in front of an RNAP would persist to slow down further RNAP elongation and eventually turn off the transcription initiation [3-6]. Meanwhile, participation of DNA gyrase that resolves the positive supercoiling would allow recovery of the transcription [6-8] (see Fig 1).

Recently, the dynamical processes of the positive supercoiling generation and gyrase binding to DNA to resolve the positive supercoiling have been suggested to directly contribute to the bacterial transcription bursting [6]. The transcription bursting had been reported for individual *E. coli* cells [9], as gene ON and OFF events were recorded from real-time transcription activity measurements. Accordingly, one could attribute the gene transcription ON to OFF transition to relatively slow gyrase unbinding or disassociation from the DNA followed by fast supercoiling accumulation, while assign the OFF to ON transition to slow gyrase binding or association onto the DNA along with fast supercoiling releasing. As the gyrase binding and unbinding events are usually slow (with characteristic time $\sim 10^3$ s), the above scenario is consistent with a two-state model [10, 11], in which the gyrase bound and unbound states are assigned to the gene ON and OFF periods, respectively.

However, one can find that the transcription ON and OFF status do not necessarily correspond to the respective gyrase bound and unbound states to DNA, as the supercoiling accumulation and release can also proceed slowly (lasting from $\sim 10^2$ s to 10^3 s) as well as in multiple kinetic steps. For example, when there is no gyrase bound to the DNA (treated as OFF in the two-state model), the transcription elongation can still proceed for a while (appear as ON in reality), during which the positive supercoiling gradually builds up and slows down the transcription activities until a final shut down of the activities. The corresponding process may take up to minutes over and do not reduce to a single kinetic event such as the gyrase unbinding transition in the two-state model. Meanwhile, gyrase can bind to DNA and once it binds and reacts, the supercoiling accumulation stops (treated as ON in the two-state

1
2
3 model). However, the transcription cannot turn ON immediately upon the gyrase
4 reaction, as it may still take several minutes for the accumulated supercoiling to fully
5 release, so that the transcription activities only gradually recover toward the original
6 level. In brief, the two-state model does not work well when the supercoiling
7 accumulation and relaxation also proceed slowly, comparable to the gyrase binding
8 and unbinding events. In such cases, a multi-state model is demanded to correctly
9 characterize the kinetic features.
10
11
12

13
14 In this work, we provide a quantitative framework to accommodate in general that the
15 supercoiling accumulation and releasing take place gradually and via multiple steps.
16 To do that, we constructed a multi-state transcriptional bursting model, in which each
17 configuration of the transcription system is characterized by the gyrase bound status
18 as well as an accumulated supercoiling density level on DNA, which presumably
19 increases one level at a time for each transcript production and decreases one by one
20 as well during the supercoiling releasing. In the model, the mRNA production
21 proceeds with time-dependent elongation and initiation rates, which are determined
22 by the supercoiling density level. Overall, the supercoiling accumulation and release
23 are regulated by the gyrase binding and unbinding events at constant rates (see **Fig 2**).
24 We abolished the assumptions in the two-state model that requires only one slow
25 transition to be dominant to switch between the gene ON and OFF periods. Current
26 multiple-state model is similar to a recent development where stepwise supercoiling
27 accumulation is also explicitly modeled and simulated to address mechanical bounds
28 to transcription noises [12]. Nevertheless, in that model, immediate supercoiling
29 release was employed, while the transcription kinetic was modeled without explicitly
30 considering the gyrase association/dissociation events. A biophysical model was also
31 built recently to take into account the supercoiling energy state of the transcription
32 [13], focusing on the promoter impacts and correlated gene expression within a
33 supercoiling domain. In addition, a general framework of stochastic transcription has
34 been built to address both the uncorrelated transcription events and bursting behaviors
35 [14]. Besides, the bursting transcription is suggested to lead to protein localization to
36 facilitate target search in the transcription regulation, according to another recent
37 modeling work [15].
38
39
40
41
42
43
44
45

46 In particular, we consider a battery of RNAPs forming elongation traffic on DNA, as
47 it is an efficient way to achieve the supercoiling regulation when there are only a
48 limited amount of gyrase molecules present in the cell [8]. The multiple RNAPs can
49 elongate in synchrony on average, so that the positive supercoiling generated in front
50 of a trailing RNAP can be immediately canceled by the negative supercoiling
51 produced behind a leading RNAP downstream in the traffic. In that case, a battery of
52 RNAPs move in tandem and only accumulate net positive supercoiling in front of the
53 first leading RNAP, so that only one gyrase molecule at a time rather than several are
54 needed to resolve the accumulated supercoiling [8]. Meanwhile, the negative
55 supercoiling produced behind the very last RNAP in the traffic can be resolved by
56 Topo I that is comparatively abundant. Within this context, one might expect that
57
58
59
60

multiple RNAPs moving in tandem would demonstrate similar or additive behaviors over individual RNAPs. Nevertheless, we show that a battery of RNAPs promotes both the mRNA and supercoiling accumulation, so that transcription noises are amplified and the transcription bursting becomes highly significant.

To model the inhibition impacts of the supercoiling on the RNAP elongation and initiation, we considered that the supercoiling generates tension on DNA to slow down both the elongation and initiation, with the initiation being impacted more significantly than the elongation. Recent measurements showed that the transcription initiation could be fully stopped while the elongation persisted at a low rate under the positive supercoiling inhibition [6]. Early studies had also indicated that the transcription initiation is sensitive to the tension on DNA [16], while the elongation rate is not highly force sensitive for T7 RNAP as well as *E. coli* RNAP [17-20]. The tension responses thus allow an existing RNAP traffic to continue elongating albeit slowly on DNA while no further RNAP transcription initiation is supported.

In this work, we first describe how the multi-state transcriptional bursting model was constructed for a single RNAP with repetitive runs of the transcription, along with analytic solutions of the model in the steady state condition. Next we utilized this model to simulate stochastically on how multiple RNAP molecules are loaded onto DNA and elongate in tandem for the same gene transcription. We chose the fast elongating T7 RNAP and the comparatively slow *E. coli* RNAP as two representative systems, which have also been directly monitored in the recent transcriptional bursting study, both in *vitro* and in *vivo* [6]. Consequently, we are able to show how the transcript productions along with the fluctuations are impacted by the supercoiling regulation for a battery of the RNAPs transcribing together on short and long DNA, respectively, based on the multi-state model.

Methods & model construction

i. Transcription and supercoiling accumulation simulation setup

The transcription process includes initiation, elongation, and termination (see **Fig 1A** and **B**). For simplicity, one may treat the initiation as one step, with an effective rate of k_{init} . In our analytic model construction (see **Fig 1A** and **Supplementary Information** or **SI**), the overall transcription was treated as one effective step. In the numerical simulation, however, detailed steps in the initiation and elongation were modeled: The promoter binding of an RNAP from free solution (with forward and backward rates of k_{pc} and k_{cp}), a reversible close-to-open transition of the promoter along with formation of a transcription bubble (with forward and backward rates of k_{co} and k_{oc}), and the RNAP complex together with the transcription bubble undergoing a series of conformational transitions via scrunching, abortive cycling, and escaping to elongation (see **Fig 1B**)[21-23] (with detailed kinetics found in [21]). The mRNA is then produced during the elongation (at a rate of k_e) until termination or towards the end of DNA (with a dissociation rate k_d), and the length of gene (L) is usually set to

hundreds to thousands of base pairs.

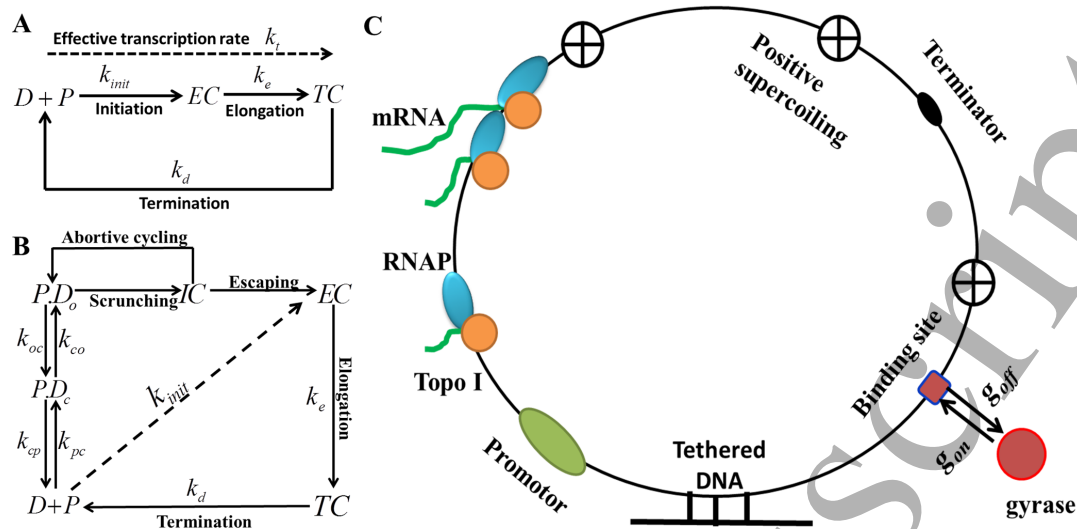


Fig 1 (A) A simplified transcription scheme including initiation, elongation, and termination. D , P , EC , and TC refer to DNA, RNAP, the elongation complex, and the termination complex, respectively. The effective initiation rate, the elongation rate, and the termination/dissociation rate are denoted as k_{init} , k_e , and k_d , respectively, while k_t refers to an overall effective rate of transcription. These rates were used in the analytic model shown in SI. (B) A complete RNAP transcription scheme including additional steps in initiation, elongation, and termination. $P.D_c$, $P.D_o$, and IC refer to the closed RNAP-DNA complex, the open complex, and the initiation complex, respectively. k_{pc} , k_{cp} , k_{co} and k_{oc} are the RNAP binding rate, RNAP unbinding rate, DNA bubble opening rate, and its closing rate, respectively. (C) The schematics of the positive supercoiling accumulation during transcription on a tethered DNA loop. The green, orange, blue, black, and red ellipsoids represent the promoter, Topo I, RNAP, terminator, and gyrase. The green line shows the mRNA in production. The black circle with the plus sign inside and the red square are on behalf of the positive supercoiling and the gyrase binding site, respectively. The gyrase binding and unbinding rates are denoted as g_{on} and g_{off} , respectively.

Studies had shown that the accumulation of positive supercoiling in front of an elongating RNAP inhibits the transcription, while the gyrase enzyme binding and action onto DNA release the positive supercoiling (see **Fig 1C**), in particular, reduce the writhe number for two during each enzymatic cycle [24-26]. Besides, the elongating RNAP also produces negative supercoiling behind, which can be quickly resolved by Topo I that may interact directly with RNAP [27] and populate abundantly in the *E. coli* cell [6, 28] (see **Fig 1C**). Otherwise, the negative supercoiling produced upstream of a leading RNAP can also be canceled by the positive supercoiling produced downstream of a trailing RNAP in the RNAP traffic, prior to the Topo I binding.

The *in vitro* experiments for single T7 and *E. coli* RNAP transcribing repetitively on the circular DNA template were actually conducted in three conditions (see Fig 4 in ref [6]): in the absence of Topo I and gyrase, in the presence of Topo I and gyrase;

and in the presence of Topo I only. There was no transcription slowing down nor bursting in the first two conditions. Only in the third case, however, the transcription was suppressed, revealing the substantial role of the positive supercoiling. In the experiment, the transcription initiation slowing down and recovery after adding the gyrase lasted for ~ 6000 s and 3000 s (see Fig 5B in ref [6]), respectively. However, the gyrase binding from bulk takes ~ 1000 s at the corresponding condition ($g_{on} = \tilde{g}_{on}[G]$ with $\tilde{g}_{on} = 10^4 \text{ M}^{-1}\text{s}^{-1}$ and the solution gyrase concentration $[G] \sim 100$ nM), while the dissociation of the gyrase from DNA also takes ~ 1000 s ($g_{off} = 10^{-3} \text{ s}^{-1}$)[6]. Hence, there must be other events that account for a significant amount of time, which we propose as the slow accumulation of the positive supercoiling and the gradual release of the accumulated supercoiling.

To quantify the positive supercoiling accumulation on the DNA, we count the supercoiling density level additively upon each transcript production, when the DNA loop or domain is tethered under a topological constraint and there is no gyrase bound to the DNA. The supercoiling density on the DNA with a linking number Lk_0 in the relaxed state is defined as

$$\sigma \equiv \Delta Lk / Lk_0, \quad (1)$$

in which the linking number Lk is counted as the sum of a DNA helical twist number Tw and a coiling or writhe number Wr

$$Lk = Tw + Wr. \quad (2)$$

In the relaxed state, the writhe number $Wr_0 = 0$, so that $Lk_0 = Tw_0 = L/10.5$, e.g. for the B-form DNA of length L .

For the downstream DNA under the topological constrain at the end, the linking number change upon the RNAP action is $\Delta Lk = l/10.5$ for a transcript of length l . Hence, upon production of each mRNA transcript of length l ($l \leq L$), one has

$$\sigma_l = l/10.5 / Lk_0 = l/L. \quad (3)$$

In accumulation, we obtain the overall supercoiling density level as $\alpha = \sum_{i=1}^{i_{\max}} \sigma_i$ for the multiple transcript production, where i_{\max} is the maximum number of transcripts being generated in the absence of the gyrase association.

As the positive supercoiling is built up in front of RNAP to shrink the length of the

DNA that is either tethered or with the two ends restrained, we consider that the tension built up along DNA impedes the RNAP translocation and ultimately slows down the elongation or initiation. Dynamic impact from supercoiling propagation along DNA has not been considered yet in current model. We assumed that both the initiation and elongation rates (as well as the effective transcription rate) are determined only by the accumulated supercoiling density level α on the DNA as defined above, and these rates decrease linearly with α for multiple runs of the transcription. A close-to-linear dependence of the transcription rate on the supercoiling accumulation has actually been demonstrated in the recent biophysical modeling [13]. In addition, it has been shown that the positive supercoiling can slow down T7 or *E. coli* RNAP elongation while fully stop the transcription initiation [6]. Hence, when we separately treated the initiation and elongation processes in the numerical simulations (described below), we assumed that the effective initiation rate k_{init} would drop all the way to zero upon the positive supercoiling accumulation, while the elongation rate k_e would be lowered to a small but non-zero value (k_e^{sm}).

ii. Construction of a multi-state transcription-bursting model for single RNAP

First, we considered the case when there is only one RNAP during transcription. As the gyrase dissociates from DNA (at a rate g_{off}), the supercoiling density increases by one level upon each full-length transcript production. Hence, the supercoiling accumulation rate can be equal to the effective production rate of the mRNA transcript, which combines the initiation and elongation together, and was assumed to decrease linearly with the number of transcripts in production

$$k_{\alpha} = k_t(\alpha^* - \alpha) / \alpha^*, \quad (4)$$

with k_t the transcription rate in the absence of the supercoiling. Note that the supercoiling level α rises along with the number of transcripts i when there is no gyrase bound on the DNA. Once the supercoiling level reaches to a maximal value at α^* , the transcription activity suspends. Note that when we treated the initiation and elongation separately in the numerical simulations, only the transcription initiation but not the elongation suspends at $\alpha = \alpha^*$.

Consequently, one sees that the supercoiling level increases in synchrony with the mRNA production in the absence of the gyrase. Once the gyrase binds onto DNA, the mRNA production can then proceed without coupling to the supercoiling accumulation; instead, the accumulated supercoiling starts releasing at a rate of g_e , as being estimated below. The detailed scheme of the multi-state model is presented in **SI Fig S1**.

For T7 RNAP transcribing on the 12 kbp DNA template, e.g., the *in vitro* experiment recorded that the transcription initiation stops after generating 9 transcripts, and recovers back ~ 2000 s after adding gyrase in solution (see Fig 5B in ref [6]). To count from the initiation *off* status, one has $\alpha=9$ at $t=0$. From $t=0$ to 1000 s on

average, gyrase has not yet bound to DNA ($g_{on}=0.001s^{-1}$ *in vitro*), and the transcript production rate was set low at $\sim 0.001 s^{-1}$ so that α further increases to 10 by e.g. $t=1000$ s. Next, from $t=1000$ to 2000 s on average, the gyrase molecule remains bound on the DNA ($g_{off}=0.001 s^{-1}$), and all the supercoiling is then released (from $\alpha=10$ to 0). Hence, the rate of releasing one supercoiling level is estimated as $g_e^0=10/1000=0.01/s$. Since g_e^0 is for a DNA length of 12,000 bp (L_0), we scaled supercoiling releasing rate for a DNA length of L as

$$g_e = \frac{L_0}{L} g_e^0. \quad (5)$$

Parameter	Symbol	value	Units	Reference
DNA loop length	L_0	12,000	bp	[6]
Effective transcription initiation rate	k_{init}	0.1~0.2	s^{-1}	<i>estimated</i>
T7 RNAP elongation rate	k_e	50~100	bp s^{-1}	[29]
<i>E.coli</i> RNAP elongation rate	k_e	10~20	s^{-1}	[30]
Effective transcription rate without supercoiling ($L=4.5$ kbp DNA)	k_t	0.02 for T7 0.002 for <i>E.coli</i>	s^{-1}	<i>estimated</i>
Termination rate	k_d	1	s^{-1}	[31]
mRNA degradation rate	γ	0.1	min^{-1}	[32]
First-order rate constant for gyrase-DNA binding	\tilde{g}_{on}	10^4	$M^{-1}s^{-1}$	[6]
Gyrase binding rate <i>in vitro</i>	g_{on}	0.001	s^{-1}	[6]
Gyrase binding rate <i>in vivo</i>	g_{on}	0.003	s^{-1}	[6]
Gyrase dissociation rate	g_{off}	0.001	s^{-1}	[6]
Supercoiling releasing rate for one density level and $L_0=12$ kbp DNA)	g_e^0	0.01	s^{-1}	<i>estimated</i>

Table1 Parameter values based on references or estimation.

The key kinetic parameters are summarized in **Table 1**, while additional parameters can be found in **SI Table S1**.

In **SI**, we show the chemical master equation for the above multi-state model, and then use the generating function method [33] to solve the equation at the steady-state condition. Consequently, the interested quantities including the average number of mRNA ($\langle m \rangle$), the Fano factor (*Fano*)[34], and the effective duty cycle ratio (*DCR*)[35] in the single RNAP transcription case were obtained.

iii. The multi-state transcription-bursting model for RNAP traffic

Then we implemented the multi-state model to describe a battery of RNAPs transcribing in traffic conditions, as one RNAP after another initiating from a same promoter and then elongating in tandem [8]. In between any two adjacent RNAPs on the DNA, the locally generated positive and negative supercoiling cancel each other. In a typical case, we considered that Topo I binds (e.g. $\sim 0.1/s$ to $0.01/s$) much more frequently than the gyrase ($g_{on} \sim 0.001/s$), but less frequently than the initiation of an individual RNAP ($k_{init} \sim 0.1/s$), and only bind to the upstream of the last RNAP in the traffic to resolve the negative supercoiling. In current setting, the initiation process usually lasts about several seconds (i.e. $5\sim 10$ s on average), Topo I binding thus happens after several RNAPs have been loaded onto the promoter for the transcription initiation. Indeed, prior to the Topo I binding, the negative supercoiling generated upstream to an elongating RNAP loaded last in the traffic might also assist the promoter opening to facilitate the next RNAP initiation.

Meanwhile, we still assume that the transcription initiation and elongation rates are mainly regulated by the tension on the DNA, which can be largely determined by the overall supercoiling density level α . Hence, even though the positive supercoiling is accumulated only in front of the very leading RNAP, due to the tension generated on the DNA, all elongating RNAPs can be slowed down with k_e dropping simultaneously. Similarly, the effective initiation rate k_{init} drops as the supercoiling density or DNA tension builds up, until a full suspension of the initiation. A summary schematics of the transcription rate changes upon the supercoiling accumulation and release is shown in **Fig 2A**, while the simplified schemes of the multi-state model for the single RNAP and traffic cases are provided in **Fig 2B** and **C**, respectively.

In the RNAP traffic, although individual RNAP elongates at the same rate, on average, there is still some chance that two RNAPs collide stochastically. We consider two types of collisions: (i) For the viral T7 RNAP which does not usually pause, a trailing RNAP can kick a leading RNAP off the DNA track if the leading one slows down and gets in the way of the trailing one [36]; (ii) For the *E.coli* RNAP, a trailing RNAP likely assists a pausing RNAP in front to recover back to the elongation [37]. We recorded the number of simultaneously elongating RNAPs on the DNA as the

working #RNAP, which is determined by the length of transcript l , the effective rates of initiation $k_{init}(\alpha)$ and elongation $k_e(\alpha)$ at a supercoiling level α , as well as by the pausing interval time τ_{pause} if there is any (pause may occur during elongation of *E.coli* RNAP with $\tau_{pause} \sim 2$ s). Hence, the average number of working RNAP can be estimated by

$$\langle \#RNAP \rangle = l / [(1/k_{init}(\alpha) + \tau_{pause})k_e(\alpha)], \quad (6)$$

with the effective rates of initiation and elongation determined by the supercoiling density level as

$$k_{init}(\alpha) = k_{init}(\alpha^* - \alpha) / \alpha^*, \quad (7)$$

and

$$k_e(\alpha) = k_e(\alpha^* - \alpha) / \alpha^* + k_e^{sm}. \quad (8)$$

Note that now the maximal supercoiling level can reach up to $\alpha^{\max} = \alpha^* + Np$ before the gyrase binds, in which Np is the number of RNAPs left on the DNA at $\alpha = \alpha^*$. That says, even though the transcription initiation stops at $\alpha = \alpha^*$, there can be Np RNAPs left on the DNA, which have been loaded prior to the transcription initiation stall and can continue transcribing until the termination. Comparing with the single RNAP case (see **Fig 2B**), the release of supercoiling or recovery of the transcription initiation takes a longer time on average in the traffic case (**Fig 2C**). Note that in this work, we attributed the gene *off* status to those transcription configurations with $\alpha \geq \alpha^*$, i.e., when the positive supercoiling fully turns off the transcription initiation; otherwise, as long as $\alpha < \alpha^*$, the transcription status remains *on*.

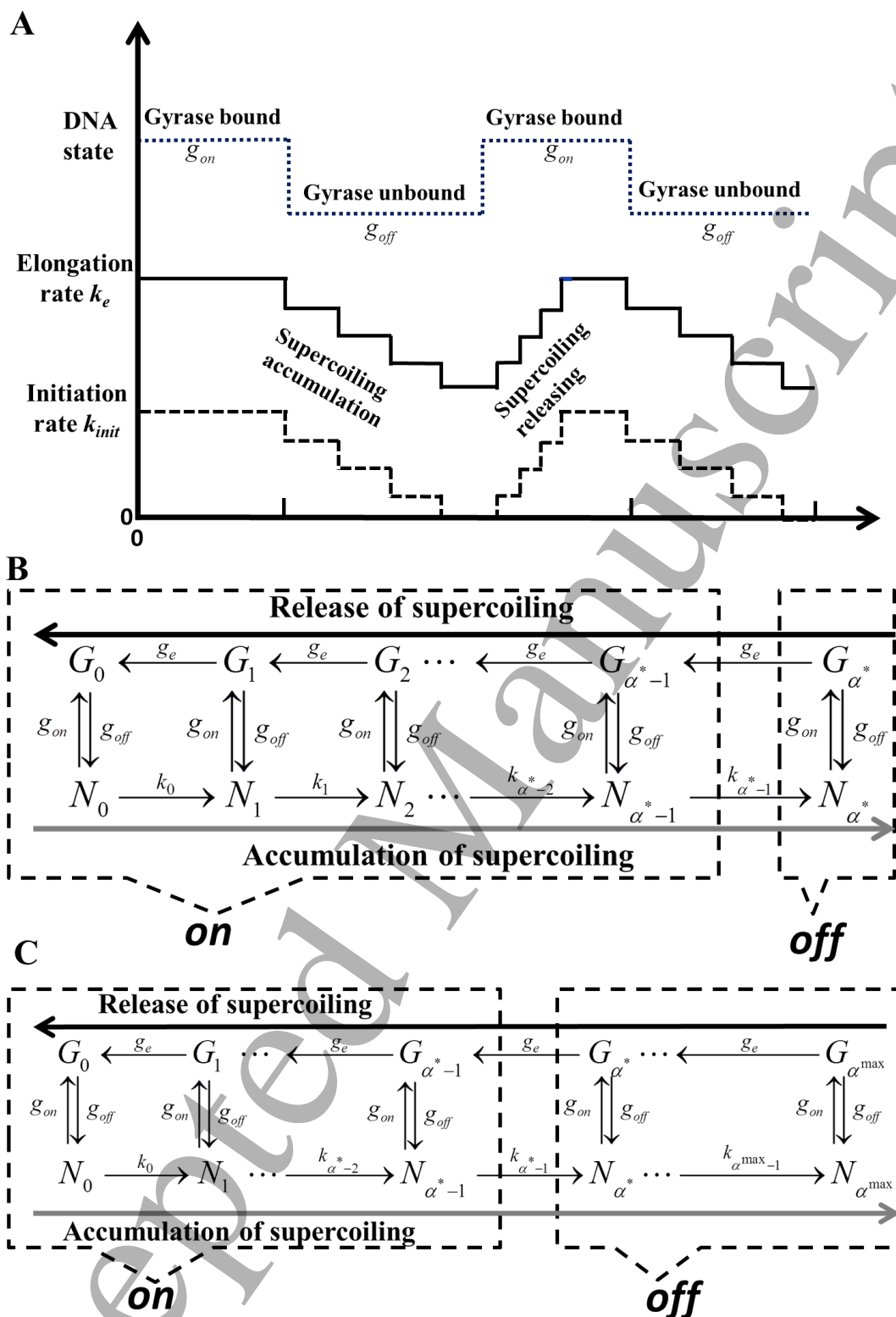


Fig 2 A summary schematics of the multi-state transcription-bursting model for both the single RNAP and traffic case. The changes of the effective transcription initiation rate (k_{init}) and the elongation rate (k_e) due to the positive supercoiling accumulation and relaxation during an RNAP transcription are shown in (A), in the presence of the gyrase binding and unbinding (at rates of g_{on} and g_{off}). The simplified schemes of the multi-state

transcription-bursting model for the single RNAP (B) and the RNAP traffic case (C) are also shown. The top and bottom layers represent the gyrase bound (G) and unbound (N) status, respectively, so that the switching in between the two status proceeds at g_{on} and g_{off} . Without the gyrase bound or N , the supercoiling accumulates along with the transcript production at a rate of k_{α} , with α^* the maximum supercoiling level formed in the single RNAP case; in the traffic case, there are still Np RNAPs left on the DNA at the initiation stall ($\alpha = \alpha^*$), accordingly, the maximum supercoiling level reaches to $\alpha^{\max} = \alpha^* + Np$. Upon the gyrase binding or G , the supercoiling releases stepwise at a rate of g_e .

iv. Numerical simulations on the RNAP traffic under supercoiling regulation

We use T7 and *E.coli* RNAPs as two representative model systems to show the multi-state transcription-bursting model. T7 RNAP can elongate comparatively fast (up to 100-200 nt/s) during the elongation [29]. *E. coli* RNAP elongates slowly, and can pause or backtrack from time to time [38]. For simplicity, the initiation kinetics of the two RNAP species was treated similarly as from T7 RNAP in our simulation [21]. The particularly slow initiation, e.g., of the *E. coli* RNAP, was then considered similar to the single RNAP transcription case examined in *ii*. As mentioned above, we assume that the collision between two *E.coli* RNAPs leads to a velocity (i.e., the elongation rate) switch between the two RNAPs, while the collision between two T7 RNAPs causes the leading RNAP to drop off the track.

In this work, we used the Kinetic Monte Carlo (KMC) algorithm [39] to simulate the RNAP transcription traffic. We simulated for the RNAP transcription, without the supercoiling first, and then in the presence of the supercoiling accumulation and releasing, according to the reaction schemes in **Fig 2C**. By default, we let the transcription initiation stop at a supercoiling density level of $\alpha^* = 4$. To compare, we used a short gene or transcript length (~ 300 bp) and a long one (~ 4500 bp) in the simulation systems. The model parameters are provided in **Table 1** and **SI Table S1**.

In the KMC simulation we grouped the states into the ‘*on*’ and ‘*off*’ sets according to the initiation status. In the ‘*off*’ set, the transcription initiation stops due to the high supercoiling density level ($\alpha \geq \alpha^*$). Otherwise, the states are in the ‘*on*’ set ($\alpha < \alpha^*$). The *DCR* is calculated as the probability of keeping the transcription initiation *on* (see detailed calculations in **SI**). Note that the *on* and *off* sets defined here, according to the transcription initiation status in the simulations, do not match exactly with the ON and OFF periods measured experimentally or directly from time series of the mRNA production.

Results

According to the multi-state transcription-bursting model presented in **Fig 2B**, we solved the steady-state chemical master equations analytically to obtain transcription characteristic of single RNAP (see **SI** and **Fig S1**). Then we conducted KMC

simulations to numerically show the steady-state characteristics in the RNAP traffic case (see **Fig 2C**), comparing the situations with and without the supercoiling regulation.

1. Characteristics of the single RNAP transcription in the multi-state model

Based on the chemical master equations of the multi-state model, we obtained analytic solutions in the steady state of single RNAP transcription. The characteristics are shown in **Fig 3** for T7 RNAP transcribing on a comparatively long piece of DNA ($L= 4500$ bp), including the average number of mRNA transcript ($\langle m \rangle$), the Fano factor (*Fano*), and the effective duty cycle ratio (*DCR*). These quantities are demonstrated by varying the gyrase binding/unbinding rate ($g_{on/off}$, 0.001/s by default), the supercoil-releasing rate (g_e , 0.027/s), the effective transcription rate (k_t , 0.02/s), the mRNA degradation rate (γ , 0.0017 /s or 0.1/min), and the supercoiling level for the initiation suspension ($\alpha^* = 4$). In the default setting, we have $\langle m \rangle \sim 6$, *Fano* ~ 3.5 , and *DCR* ~ 0.66 .

First, one can see that an increase of g_{on} for ten times (to 0.01/s) leads to about twice the amount of mRNA transcripts ($\langle m \rangle \sim 12$) along with a low value of the *Fano* (~ 1), indicating an enhanced transcription and quenched fluctuation when gyrases are abundant to allow sufficiently fast actions to remove the accumulated supercoiling. Lowering the gyrase unbinding rate g_{off} shows similar impacts. The *Fano* remains low even when g_{on} rises ($> 0.01/s$) or g_{off} drops ($< 0.0001/s$) further. On the other hand, a decrease of g_{on} for one order of magnitude (to 0.0001 /s) lowers the mRNA production close to zero while allowing a rise of the *Fano* factor (> 5), as having fewer gyrases or slower gyrase binding encourages the system to stay longer in the gyrase unbound state, with inhibited transcript productions across multiple supercoiling density levels. In comparison, a significant rise of g_{off} (e.g., to 0.01 /s) can lower both the mRNA production and the *Fano* factor, since the configuration with particularly high supercoiling level transits too fast to the gyrase unbound state, without being able to release the supercoiling. Nevertheless, the currently adopted supercoiling release rate upon the gyrase action (g_e) appears to be large enough such that a further increase of it does not improve the mRNA production, nor it leads to any decrease of the *Fano* or increase of the *DCR*. Reducing g_e , however, would significantly reduce the mRNA production, raise the *Fano*, and lower the *DCR*, making the transcription difficult and versatile.

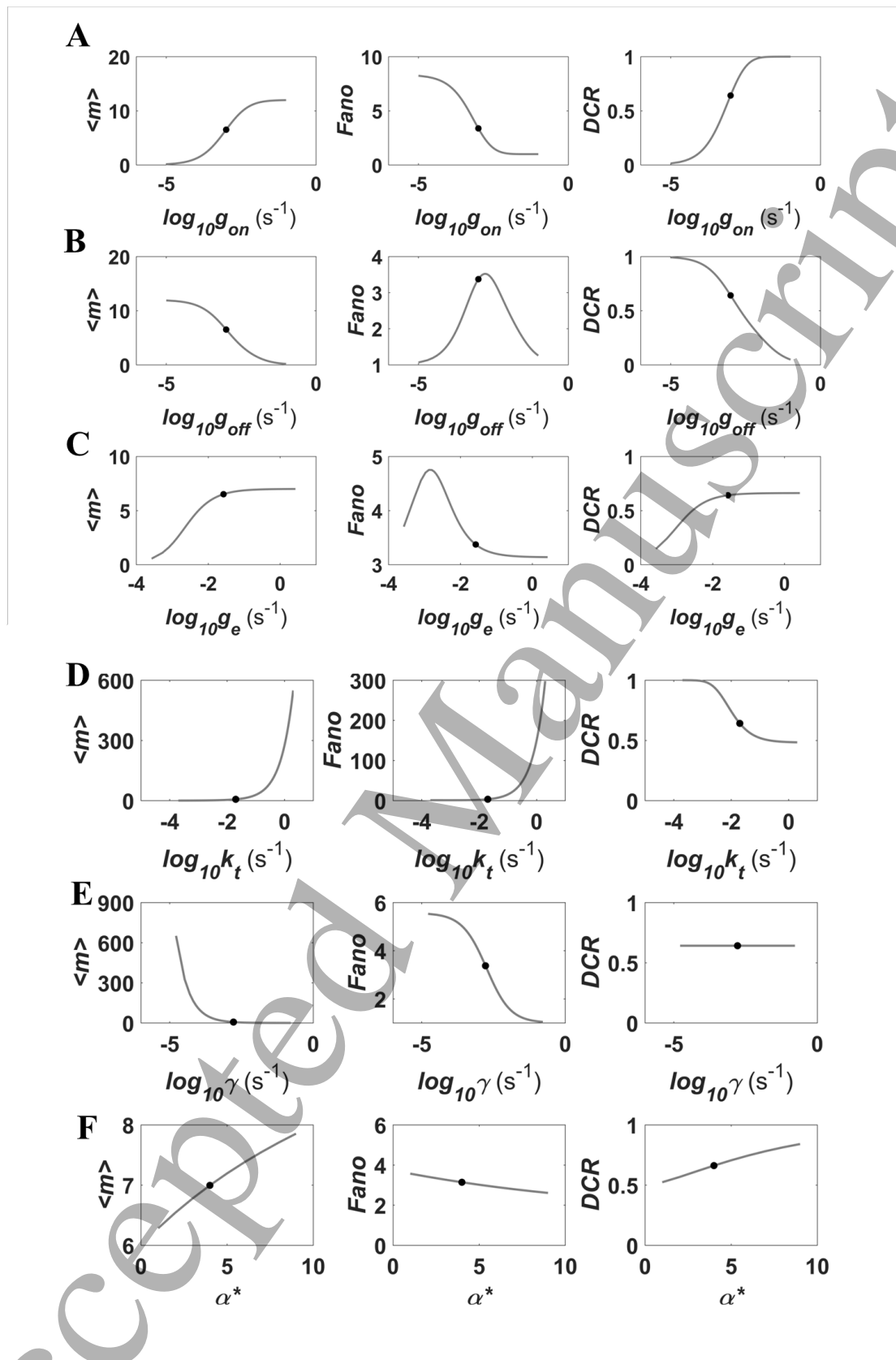


Fig 3. The steady-state characteristics in the single T7 RNAP transcription ($L=4500$ bp) as obtained analytically from the multi-state transcription-bursting model in **Fig 2B** (and **SI Fig S1**). The changes of $\langle m \rangle$, *Fano*, and *DCR* upon variations of the gyrase binding and

1
2
3 unbinding rates (A) g_{on} and (B) g_{off} , the supercoiling release rate (C) g_e , the effective
4 transcription rate (D) k_t , the mRNA degradation rate (E) γ , and the maximum supercoiling
5 level (F) α^* are presented, respectively. The values labeled by the black points were
6 calculated under the default setting.
7
8
9

10 In addition, one can see that a continuing rise of the effective transcription rate (k_t)
11 would lead to a steep increase of the mRNA production, while the *Fano* also rises
12 sharply. The *Fano* drops low as k_t reduces to very low values. Lowering the mRNA
13 degradation rate (γ) promotes both the mRNA production and the *Fano*, with no
14 impacts on the *DCR*. Finally, if one varies α^* , the maximum supercoiling density
15 level for the transcription initiation suspension, neither the mRNA production nor the
16 Fano factor changes much. However, the *DCR* increases from ~ 0.5 to approaching to
17 1 as α^* increases from 1 to 9.
18
19
20
21

22 **2. Verifying the multi-state characteristics in the time series of the mRNA** 23 **production**

24 To verify that our model captures multi-state characteristics that are experimentally
25 detectable, we recorded the duration time of the ON and OFF periods according to the
26 simulated time series of the mRNA production in our model, for both the single
27 RNAP and traffic cases. Note that the current model is intrinsically multi-state, yet
28 one could group various configurations into the *on* and *off* sets, intrinsically,
29 according to the transcription initiation status. To be compatible with experimental
30 detections, however, we determined the transcription OFF period phenomenologically
31 when there was no mRNA production within a certain time window. The time
32 window was chosen at ~ 100 s, approximately an upper bound value for the time
33 interval in between two consecutively generated transcripts during the transcription
34 ON period.
35
36
37
38
39

40 **Fig 4A and B** show the time series of the mRNA production obtained in the single T7
41 RNAP transcription and the corresponding traffic case, respectively. The DNA length
42 is $L=4500$ bp, and there are 14 RNAPs in the cell (~ 38 nM) in the traffic case. In
43 comparison, one notices that the average transcript production ON time is longer in
44 the single T7 RNAP transcription ($T_{ON}=19.5 \pm 0.9$ mins) than in the traffic case
45 ($T_{ON}=15.2 \pm 0.6$ mins); the OFF time appears shorter in the single RNAP case ($T_{OFF}=4.7$
46 ± 0.3 mins) than in the traffic case ($T_{OFF}=6.8 \pm 0.8$ mins). Note that the system
47 parameters (see **Table 1** and **SI Table S1**) were incorporated to be consistent with
48 that from the *in vitro* measurements of T7 RNAP [6], except that we set $\alpha^*=4$
49 instead of $\alpha^*=9$ then to mimic the *in vivo* condition. The observations show that the
50 RNAP traffic biases the transcription into the OFF period, and the transcription bursts
51 appear more significant in the traffic case.
52
53
54
55
56
57
58
59
60

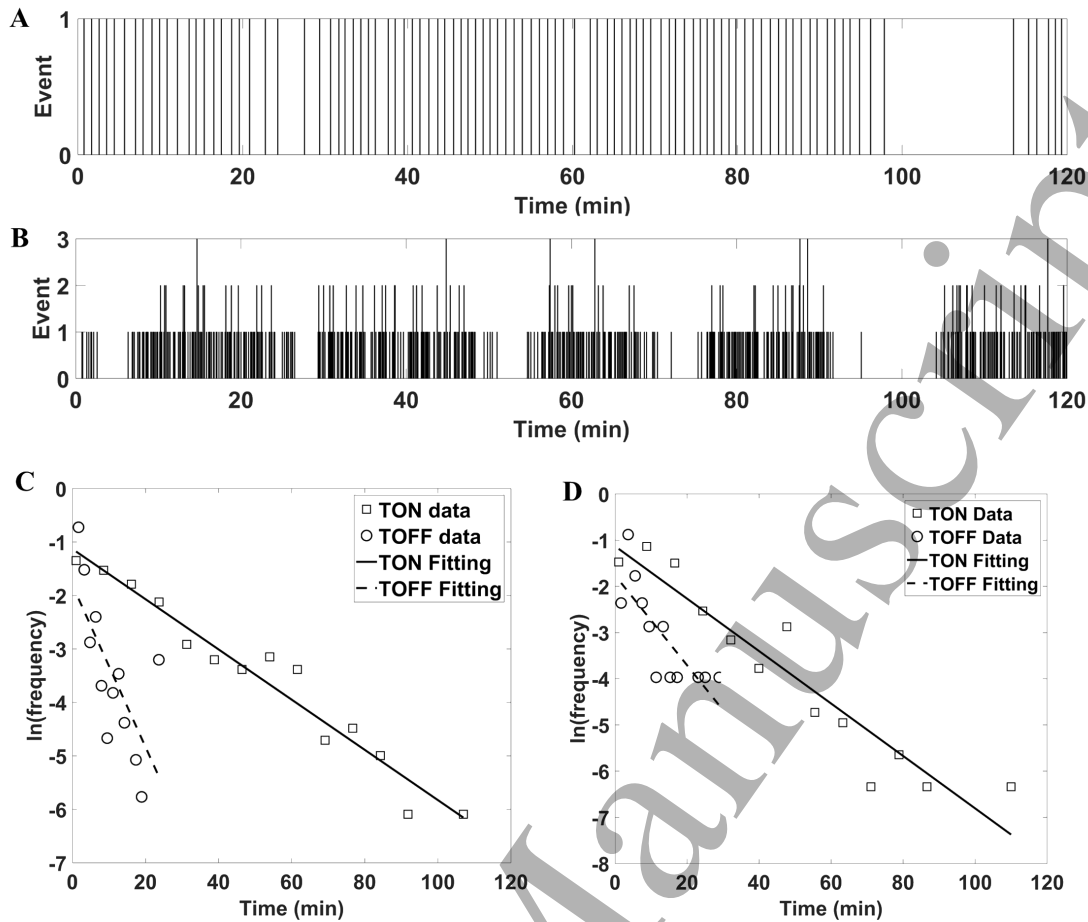


Fig 4. Measuring the ON and OFF duration times in the simulated time series of the mRNA production. The time series in the transcription of single T7 RNAP and RNAP traffic (with 14 RNAPs in the cell) are shown in (A) and (B), respectively. The DNA length is $L = 4500$ bp and $\alpha^* = 4$. (C) The fittings of the ON and OFF duration times from the trajectories as shown in (A), with the duration time frequencies shown in logarithmic values. The R^2 of the linear fittings for the log values of frequencies of the ON and OFF times are 0.95 and 0.44, respectively, with the average duration times $T_{ON} = 19.5 \pm 0.25$ mins and $T_{OFF} = 4.7 \pm 0.17$ mins. (D) The fittings for the log values of frequencies of the ON and OFF duration time from the trajectories as shown in (B). The R^2 of the respective linear fittings are 0.89 and 0.60, with the average duration times $T_{ON} = 15.2 \pm 0.20$ mins and $T_{OFF} = 6.8 \pm 0.28$ mins (with the standard errors). The bin size used in the frequency counting is 2 minutes. 100 trajectories of 200 minutes each were used to obtain the statistics.

Notably, one sees that the distributions of the duration times of the ON and OFF periods, in particular that in the OFF period, do not fit well in the log linear fittings (see **Fig 4C** and **D**), which indicate that the underlying processes deviate from the Poisson process, or say, the two-state model do not work well for the above transcription activities. The results thus confirm that the simulated time series from the current model contain multi-state characteristics easy for experimental detections.

3. Supercoiling regulation increases the variations of the number of working

RNAPs for long DNA transcription

In the RNAP traffic case, the number of RNAPs working simultaneously on DNA, i.e., the working #RNAP, is a stochastic variable, which is affected by the RNAP concentration ($[RNAP]$) in the cell, how fast an RNAP opens the promoter and then escapes to elongation (effectively by k_{init}), by how fast the RNAP elongates (k_e) along with the DNA length (l), and also by the dimension of the RNAP (r). Without the DNA supercoiling, the working #RNAP demonstrates a single peak distribution (gray histograms in **Fig 5**). The higher the $[RNAP]$ in the cell, the larger the values of k_{init} and l , the more the working RNAPs on the DNA. On the other hand, the larger values of k_e and r lead to the fewer working RNAPs.

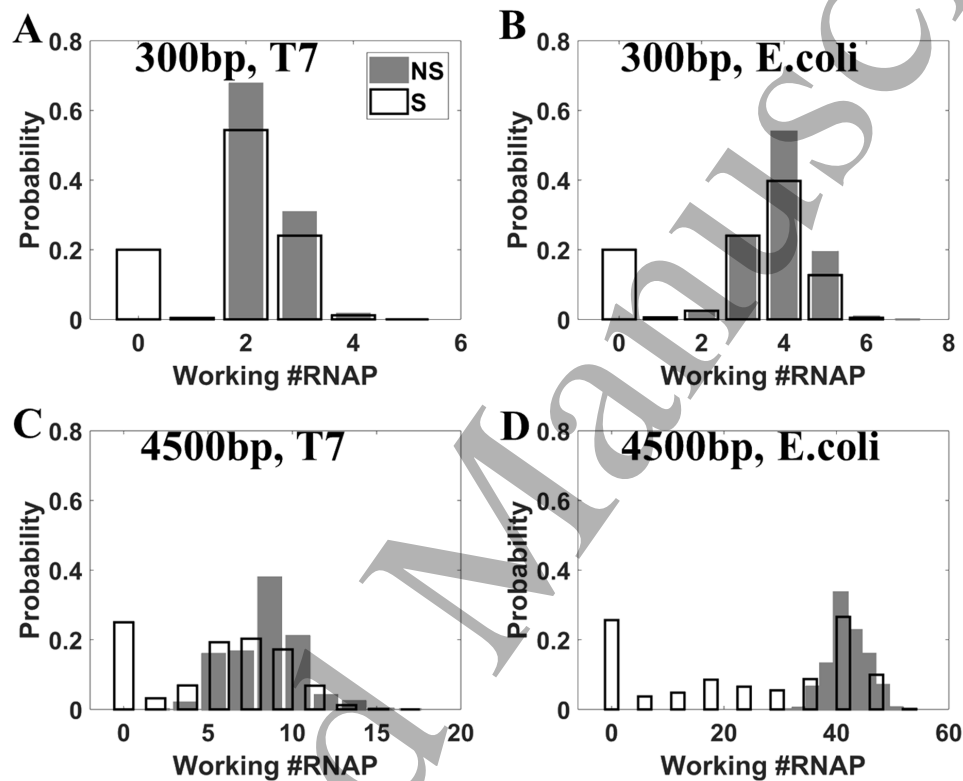


Fig 5 The distributions of the working #RNAPs on DNA ($[RNAP]=270$ nM, or ~ 100 RNAPs in cell), without the supercoiling (NS, gray bars) and with supercoiling (S, black-line bars) for four settings: (A) 300-bp DNA, T7 RNAP; (B) 300-bp DNA, *E.coli* RNAP; (C) 4500-bp DNA, T7 RNAP; (D) 4500-bp DNA, *E.coli* RNAP.

In the presence of the supercoiling accumulation and releasing, the distributions of the working #RNAP expand to low value ranges. Except for a peak at zero (i.e., in the OFF period), the distribution expansion is not significant for the short or fast DNA transcription (see **Fig 5A-C**). In the slow transcription with comparatively long DNA, e.g., $L=4500$ bp for the *E. coli* RNAP, the working #RNAP without the supercoiling is $\sim 40 \pm 5$, while the distribution expands to a full range of < 45 under the supercoiling regulation (see **Fig 5D**). Note that in the default setting, there are 100 RNAPs per cell (or $[RNAP] \sim 270$ nM) in our simulation. It turns out that only a portion of these RNAPs are able to be simultaneously working on the DNA, i.e., the maximum

working #RNAP is still significantly lower than the total #RNAP in the cell. In the presence of the supercoiling accumulation, there would be fewer RNAPs loaded onto DNA due to the initiation inhibition, though the elongation inhibition would accommodate slightly more RNAPs simultaneously working. Overall, a significant variation of the working #RNAP appears under the supercoiling regulation in the long DNA transcription.

4. The RNAP traffic increases the mRNA production and also enhances the supercoiling accumulation to inhibit the mRNA production

As expected, the average #mRNA produced ($\langle m \rangle$) increases with the #RNAPs in the cell or [RNAP], but soon reaches a plateau once the working #RNAP on DNA does not increase any further (see Fig 6). T7 RNAP transcribes much faster than *E. coli* RNAP, hence, leading to higher $\langle m \rangle$. The presence of the supercoiling inhibits the mRNA production particularly in the RNAP traffic case, as long as there are more than ~ 10 RNAPs in the cell.

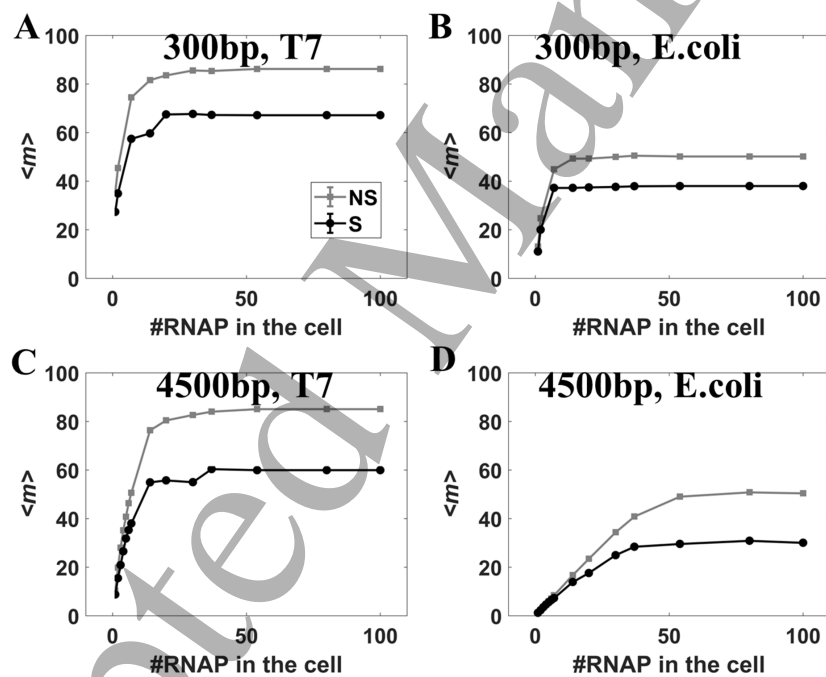


Fig 6 The impacts of RNAP traffic on the average mRNA production $\langle m \rangle$ in the no supercoiling case (NS, gray curve) and the supercoiling case (S, black curve) for four settings: (A) 300-bp DNA, T7 RNAP; (B) 300-bp DNA, *E.coli* RNAP; (C) 4500-bp DNA, T7 RNAP; (D) 4500-bp DNA, *E.coli* RNAP. 100 trajectories were used with standard errors provided. Specifically, one notices that in the absence of the supercoiling, the same RNAP species transcribing short and long DNA leads to the same amount of mRNA or $\langle m \rangle$ at the steady state, despite different working #RNAP in the short and long gene cases

(e.g., 2 and 10 T7 RNAPs on the short and long DNA at saturation and both produce ~ 75 transcripts; 4 and 40 *E. coli* RNAPs on the short and long DNA and both produce ~ 50 transcripts). This is because the same species of RNAPs use the same amount of the initiation time on average, or say, the mean duration time between two adjacently produced transcripts keeps the same for the same RNAP species. The presence of the supercoiling, however, inhibits the mRNA production a bit more and thus leads to a slightly lower $\langle m \rangle$ in the long DNA transcription, owing to the higher level of supercoiling accumulation on the long DNA.

5. RNAP traffic significantly enhances the noises in the presence of supercoiling

For the stochastic production of mRNA, one can measure the Fano factor as the ratio between the variance and the average of #mRNA, so that to quantify the fluctuation level and determine how much the production resembles the Poisson process. In case that the transcription is modeled by a single rate-limiting transition, as for the Poisson process, the *Fano* equals to 1. In the simulations of stepwise transcription initiations followed by repetitive elongation cycles (see **Fig 1B**), without considering the supercoiling, one obtains the *Fano* consistently smaller than 1 no matter in the single RNAP or the traffic transcription condition (e.g. $\sim 0.5 - 0.7$ for T7 RNAP, ~ 0.5 for *E. coli* RNAP). Accordingly, the transcript mRNA production follows the sub-Poissonian distribution.

In the presence of the supercoiling, however, the *Fano* can become much larger. The *Fano* also increases with the [RNAP] in the cell until it reaches a plateau, as the working #RNAP on DNA cannot increase any more (see **Fig 7A**). Besides, one notices that the longer the DNA, and the faster the transcription, the larger the *Fano* converges to (e.g., 6 and 8 for the short and long DNA transcription by T7 RNAP, respectively; 5 and 7 for the short and long DNA transcription by *E coli* RNAP), as the supercoiling accumulation becomes more significant. We also demonstrate the *Fano* vs. $\langle m \rangle$ relationship in **Fig 7B**. One can see that the Fano factor always increases with the average #mRNA in production, as the #RNAPs increases in the cell and becomes then saturated on the DNA.

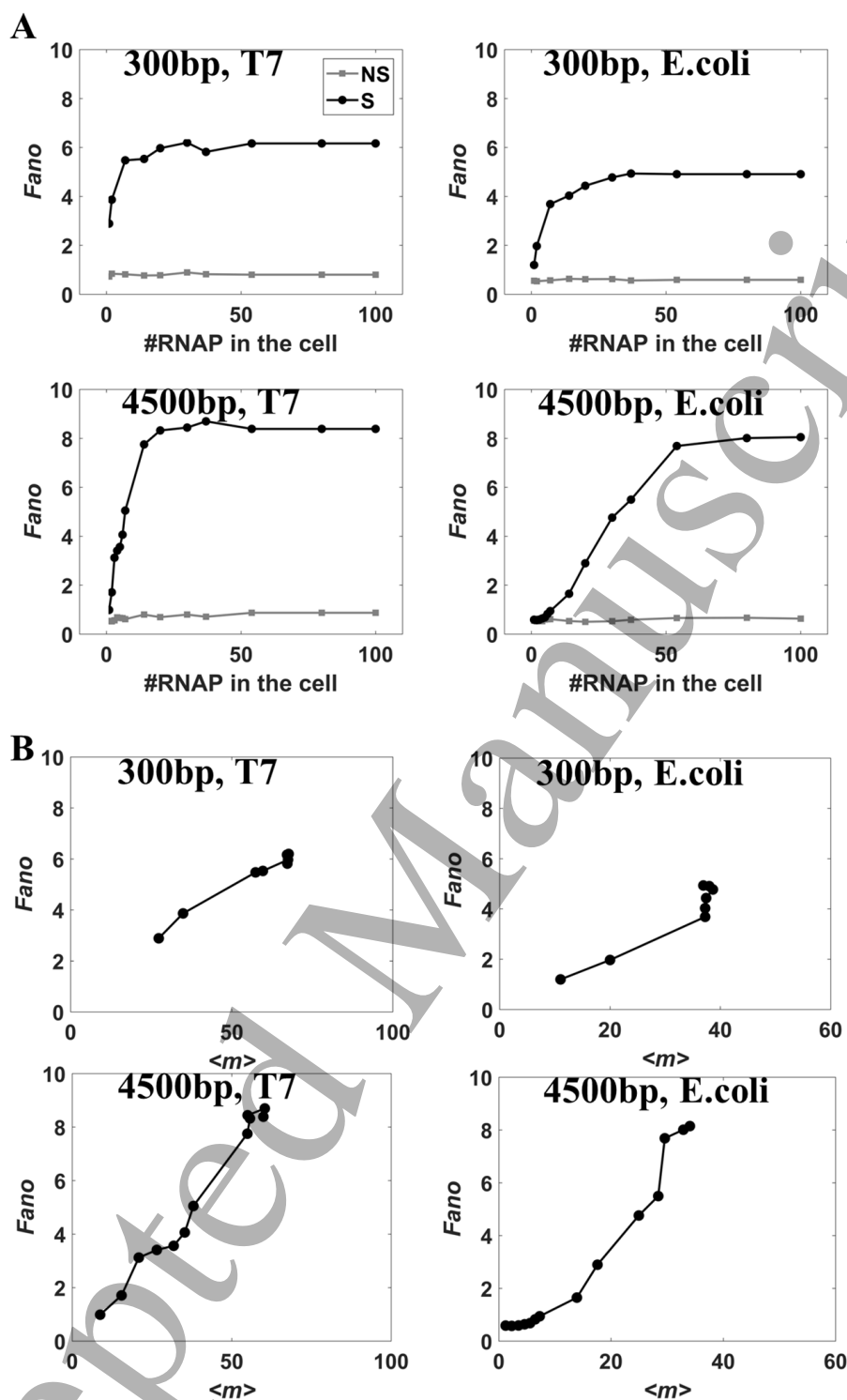


Fig 7 (A) The RNAP traffic impacts on the Fano factor in the no supercoiling (NS, gray) and the supercoiling case (S, black) for four settings: 300-bp DNA, T7 RNAP; 300-bp DNA, E.coli RNAP; 4500-bp DNA, T7 RNAP; 4500-bp DNA, *E.coli* RNAP. **(B)** The relationship between the *Fano* and $\langle m \rangle$ (as obtained in Fig 6, i.e., by increasing the #RNAP in the cell) in the corresponding settings with the supercoiling regulation.

6. RNAP traffic on long gene transcription bias the transcription to the transcription initiation *off* status

For the RNAP transcription, one can also measure the intrinsic duty cycle ratio DCR (see detailed calculations in SI), which characterizes how much percentile the RNAP engages in the transcription initiation *on* status. In the presence of the supercoiling, the DCR decreases with $[RNAP]$ before reaching to a plateau, where the working $\#RNAP$ on DNA cannot increase further. Hence, the RNAP traffic essentially biases the transcription toward the *off* status due to the enhanced supercoiling inhibition. Accordingly, the long DNA transcription would bias more toward the *off* status in the high traffic condition as a comparatively large population of working RNAPs are accommodated on the DNA (e.g. the DCR in the short DNA case is larger than $g_{on}/(g_{on}+g_{off}) \sim 0.75$, in the long DNA case becoming smaller than 0.75; see Fig 8A). When there are a small number of working RNAPs, the DCR can reach high: For example, in the case of *E.coli* RNAP transcribing $L=4500$ bp DNA, $DCR > 0.90$ for $\#RNAP < 5$ in the cell. When $[RNAP]$ keeps low, the long DNA transcription actually leads to larger DCR than the short DNA transcription, as supercoiling accumulation proceeds comparatively slower in the long DNA case.

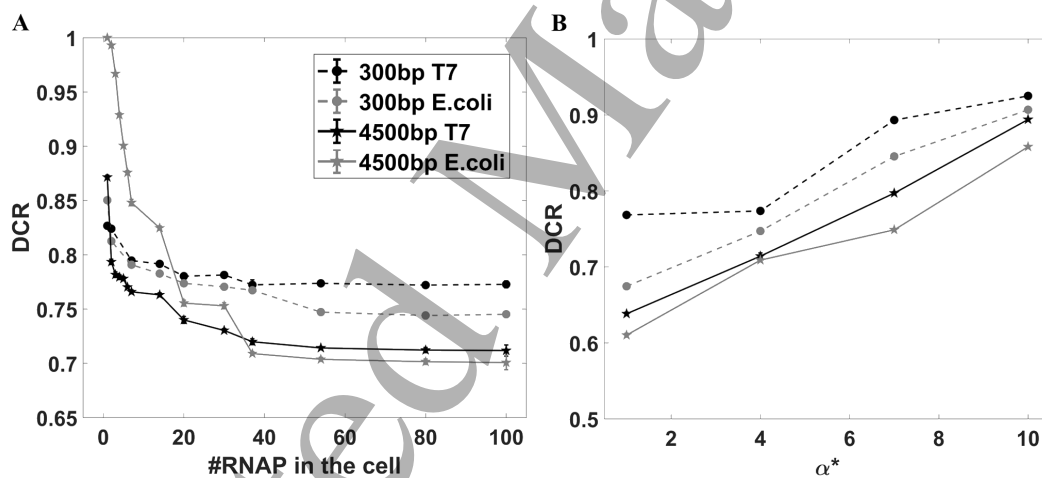


Fig 8 The variations of the duty cycle ratio DCR . (A) The DCR vs. the RNAP traffic in the supercoiling case for four settings. (B) The DCR variations with α^* in the traffic cases. The $\#RNAP$ in the cell is set at 100 or say $[RNAP] \sim 270$ nM). The standard errors of DCR for four settings were provided.

By varying α^* , the DCR obtained at different conditions change in similar trends (see Fig 8B): the larger α^* leads to the higher DCR . With the increasing of α^* , it becomes harder to accumulate high enough supercoiling level to inhibit the transcription initiation. That is to say, the less sensitive the initiation rate is to the supercoiling inhibition, the larger the bias is set toward the initiation *on*.

Discussion

In current work we developed a multi-state transcription-bursting model in order to accommodate potentially slow and stepwise supercoiling accumulation and releasing processes for bacterial transcription regulation. When topoisomerase I enzymes are present comparatively abundant, only positive supercoiling accumulates substantially in front of the transcribing RNAP(s) on the DNA that is topologically constrained. Consequently, the transcription activities are inhibited by the positive supercoiling accumulation. We consider that the transcription slowing down proceeds in synchrony with the supercoiling density building up on the DNA, which rises for one level at a time upon each mRNA transcript production. As a result, the supercoiling accumulation proceeds stepwise and takes a comparable amount of time as the RNAP elongation. The process can thus be regarded slow (e.g. from several to tens of minutes), especially for long transcript or slow elongation. In the case of high RNAP traffic, the supercoiling impacts become even more significant. The release of the supercoiling also proceeds comparatively slowly for processive gyrase actions on the DNA, e.g., over minutes for a long transcript [25]. As the timescales of supercoiling accumulation and relaxation approach to that of the gyrase binding and unbinding (e.g. minutes to tens of minutes), the two-state model that requires single slow event to dominate the gene ON/OFF switching does not work well any more. Our multi-state model accordingly accommodates the more general situation.

The roles of RNAP convoys in transcription and bursting have been concerned lately [40, 41]. According to our study, the convoy or traffic of RNAPs turns out to substantially enhance the fluctuation of the mRNA production as the transcription subjects to the supercoiling regulation. Although multiple simultaneously working RNAPs improve the mRNA production, they also promote the supercoiling accumulation to inhibit the transcription, and the inhibition becomes more significant with an increasing number of RNAPs working together on the DNA until saturation. Accordingly, the Fano factor of the mRNA production, which is boosted over one due to the transcription bursting under supercoiling regulation, can be maximally enhanced (e.g. to 5-10) for a battery of RNAPs in dense traffic.

Underlying, the supercoiling regulation can substantially enhance the variations of the working #RNAPs on DNA. The working #RNAPs at saturation on the DNA can be significantly lower than the total amount of RNAP molecules in the cell and is affected by several factors: It is controlled by how fast an RNAP is loaded and occupies on the promoter for initiation, i.e., the larger the effective initiation rate (k_{init}), the more RNAPs simultaneously work on the same DNA; it is also affected by how long the transcription elongation lasts, i.e., the larger the length of gene (L), and the lower the elongation rate (k_e), the more RNAPs can sustain on DNA. Without considering the pausing activities, one finds the average working #RNAPs scales with $L k_{\text{init}}/k_e$. In the presence of the topological constraint and supercoiling accumulation, both the rates of the initiation and elongation drop accordingly. Since the initiation appears to be more sensitive to the tension on DNA due to the supercoiling

1
2
3 accumulation, k_{init} decreases more quickly than k_e till a full initiation suspension.
4 Correspondingly, the average working #RNAP decreases upon the supercoiling
5 accumulation, while the overall distributions of the working #RNAP can be
6 significantly expanded for the long transcript or slow elongation.
7
8

9
10 Putting together, one can see that the supercoiling and RNAP traffic impact on each
11 other to regulate the overall mRNA productions and fluctuations. It can be counter
12 intuitive since a large number of RNAPs working together does not quench the
13 transcription noises. Instead, due to the correlation between the RNAP traffic and the
14 supercoiling accumulation that serves as a DNA mechanical feedback to the
15 transcription, the transcription productivities become more versatile in the traffic
16 condition. Consequently, by varying the #RNAPs on DNA or in the cell, one obtains
17 the positive correlation between the Fano factor and the average amount of mRNA in
18 the steady-state production, which turns out to be another gene-nonspecific feature in
19 the mRNA production [42]. The positive correlation between the mRNA production
20 and the Fano factor or fluctuation can also reveal by directly speeding up the
21 transcription or slowing down the mRNA degradation. Modulating only the
22 supercoiling regulation kinetics, e.g., by accelerating the gyrase association,
23 de-accelerating the gyrase dissociation with the DNA, or enabling sufficiently fast
24 supercoiling releasing, however, one would obtain improved mRNA productions with
25 quenched fluctuations. Note that the *Fano* and $\langle m \rangle$ characteristics for the single
26 RNAP transcription (in **Fig 3A**) maintain the same trends for the traffic condition
27 (results not shown).
28
29
30
31
32
33
34
35

36 For a battery of T7 or *E. coli* RNAPs transcribing in tandem considered in current
37 setting, occasional collisions due to stochasticity or RNAP pausing (*E. coli*) do not
38 seem to interfere much the overall traffic. One may actually regard a battery of
39 RNAPs in dense traffic as an integrated transcription machinery. On average, these
40 RNAPs move one behind another to avoid supercoiling building up within the pack,
41 so that only a small amount of gyrase molecules are needed to remove the positive
42 supercoiling in front of the very leading RNAP. In current model, we assume that the
43 overall tension generated on DNA under the supercoiling condition essentially slows
44 down the transcription initiation and elongation. Hence, even the positive supercoiling
45 is geometrically restricted to the very downstream region in front of the RNAP battery,
46 the tension persists all along the DNA to impact on the RNAP transcription.
47
48
49

50
51 The duty cycle ratio *DCR* turns out to be insensitive to the #RNAP in the dense traffic,
52 while in the low traffic condition, it decrease largely with an increasing #RNAP, in
53 particular, for the slow transcription of long DNA. Note that the *DCR* in current work
54 was evaluated according to the probability of the RNAP transcription initiation *on*
55 status. For a small number of RNAPs transcribing slowly to generate a long transcript,
56 supercoiling hardly accumulates soon to inhibit the transcription, hence, there is
57 almost no *off* status and the *DCR* reaches quite high (e.g. larger than 95%). Note that
58
59
60

1
2
3 the comparatively low *DCR* for the dense RNAP traffic can improve, however, with
4 an increasing value of the maximum supercoiling level (α^*) to suspend the
5 transcription initiation, which corresponds to lowering the sensitivity of the promoter
6 to the supercoiling inhibition. That says, a less tension-sensitive promoter encourages
7 a high *DCR* for the RNAP traffic machinery.
8
9

10
11 Note that some of properties demonstrated in current model rely on how the RNAP
12 elongation and initiation react to the DNA tension during the supercoiling regulation.
13 We assume that the RNAP elongation rate is less sensitive to the tension than the
14 initiation rate, according to experimental measurements so far. During an elongation
15 cycle of T7 or *E. coil* RNAP, it had been found that the translocation is unlikely a rate
16 limiting step, so that the force implementation on DNA that deters the RNAP
17 translocation cannot significantly change the overall elongation rate. On the other
18 hand, the tension on DNA appears to be easily detected by the promoter, such that a
19 comparatively small force (<10 pN) can hinder the RNAP initiation, due to the force
20 sensitive promoter opening or the RNAP 'abortive escaping'. Accordingly, in current
21 model, the elongation rate drops to a small but nonzero value at the time of the
22 initiation suspension or the *off* status. As a result, there exists a period of time during
23 which a small number of RNAPs loaded before the initiation suspension continue
24 elongating on the DNA, prior to a complete transcription OFF. The low-rate
25 elongation persisting after the initiation turning *off* can nevertheless be detected as ON,
26 due to a small amount of transcripts produced by those left RNAPs on the DNA.
27
28
29
30
31
32

33 Besides, we assume in current model that the elongation and initiation slow down
34 constantly upon each transcript production, as the supercoiling density keeps building
35 up. Indeed, how fast the supercoiling generates and propagates on DNA during the
36 transcription, how exactly an elongating or initiating RNAP reacts to the supercoiling
37 accumulation, and how exactly the supercoiling is resolved upon the gyrase action,
38 remain physically elusive. In addition, for high concentrations of topoisomerase I,
39 some of RNAPs may have negative supercoiling upstream being resolved
40 immediately, so that positive supercoiling may prevail in front of quite many RNAPs
41 in the traffic. Consequently, there can be several groups of RNAPs occupying
42 differently localized supercoiling regions on the same DNA. The supercoiling
43 regulation on individual RNAPs in a battery or convoy of RNAPs may become more
44 involved. All these aspects deserve further investigations.
45
46
47
48
49
50

51 **Conclusion**

52 By building up a multi-state model of bacteria transcription bursting, we are able to
53 describe potentially slow and stepwise supercoiling accumulation and releasing
54 processes in a general quantitative framework. In particular, we address for a battery
55 of RNAPs transcribing in tandem under the positive supercoiling regulation by
56 employing the multi-state model. It is found that supercoiling regulation enhances
57 variations of the number of RNAPs working together on DNA, so that the traffic of
58
59
60

1
2
3 RNAPs amplifies the supercoiling impacts to the transcription. Consequently, the
4 RNAP traffic promotes the mRNA production as well as enhances the mRNA
5 fluctuations, leading to the highly pronounced transcriptional bursting. The positive
6 correlation between the average mRNA production and fluctuations under the RNAP
7 traffic condition thus reveals as one of generic features in the gene transcription. In
8 comparison, modulating gyrase kinetic impacts on the DNA supercoiling may
9 improve the mRNA production while quench the fluctuations. Furthermore, the
10 RNAPs in dense traffic resemble an integrated transcription machinery with a duty
11 cycle ratio between the initiation *on* and *off* maintained low but independent of the
12 number of RNAPs. To verify current model, it is essential to physically determine the
13 supercoiling dynamics along DNA together with the mechanical responses of RNAPs
14 in the transcription bursting process.
15
16
17
18
19
20

21 Acknowledgements

22
23 This work is supported by NSFC #11775016, #11635002, and #11275022. We
24 acknowledge the computational support from the Beijing Computational Science
25 Research Center (CSRC).
26
27
28

29 References

- 30
31 [1] Borukhov S and Nudler E 2008 RNA polymerase: the vehicle of transcription
32 *Trends in Microbiology* **16** 126-34
33 [2] Buc H and Strick T eds 2009 *RNA polymerase as molecular motors*
34 (Cambridge, UK: The Royal Society of Chemistry)
35 [3] Liu L F and Wang J C 1987 Supercoiling of the DNA template during
36 transcription *Proc Natl Acad Sci USA* **84** 7024-7
37 [4] Kouzine F and Levens D 2007 Supercoil-driven DNA structures regulate
38 genetic transactions *Frontiers in Bioscience* **12** 4409-23
39 [5] Dorman C J and Dorman M J 2016 DNA supercoiling is a fundamental
40 regulatory principle in the control of bacterial gene expression *Biophysical*
41 *Reviews* **8** 89-100
42 [6] Chong S, Chen C, Ge H and Xie X S 2014 Mechanism of transcriptional
43 bursting in bacterial *Cell* **158** 314-26
44 [7] Baranello L, Kouzine F and Levens D 2013 DNA topoisomerases beyond the
45 standard role *Transcription* **4** 232-7
46 [8] Guptasarma P 1996 Cooperative relaxation of supercoils and periodic
47 transcriptional initiation with polymerase batteries *BioEssays* **18** 325-32
48 [9] Golding I, Paulsson J, Zawilski S M and Cox E C 2005 Real-Time Kinetics of
49 Gene Activity in Individual Bacteria *Cell* **123** 1025-36
50 [10] Friedman N, Cai L and Xie X S 2006 Linking Stochastic Dynamics to
51 Population Distribution: An Analytical Framework of Gene Expression
52 *Physical Review Letters* **97** 168302
53 [11] Ge H, Qian H and Xie X S 2015 Stochastic Phenotype Transition of a Single
54
55
56
57
58
59
60

- 1
2
3 Cell in an Intermediate Region of Gene State Switching *Physical Review*
4 *Letters* **114** 078101
- 5
6 [12] Sevier S A, Kessler D A and Levine H 2016 Mechanical bounds to
7 transcriptional noise *Proc Natl Acad Sci U S A* **113** 13983-8
- 8
9 [13] Bohrer C H and Roberts E 2016 A biophysical model of supercoiling
10 dependent transcription predicts a structural aspect to gene regulation *BMC*
11 *biophysics* **9** 2
- 12
13 [14] Brackley C A, Johnson J, Bentivoglio A, Corless S, Gilbert N, Gonnella G and
14 Marenduzzo D 2016 Stochastic Model of Supercoiling-Dependent
15 Transcription *Physical Review Letters* **117** 018101
- 16
17 [15] Kar P, Cherstvy A G and Metzler R 2018 Acceleration of bursty multiprotein
18 target search kinetics on DNA by colocalisation *Physical Chemistry Chemical*
19 *Physics* **20** 7931-46
- 20
21 [16] Skinner G M, Kalafut B S and Visscher K 2011 Downstream DNA Tension
22 Regulates the Stability of the T7 RNA Polymerase Initiation Complex
23 *Biophysical Journal* **100** 1034-41
- 24
25 [17] Thomen P, Lopez P J, Bockelmann U, Guillerez J, Dreyfus M and Heslot F
26 2008 T7 RNA Polymerase Studied by Force Measurements Varying Cofactor
27 Concentration *Biophysical Journal* **95** 2423-33
- 28
29 [18] Wang M D, Schnitzer M J, Yin H, Landick R, Gelles J and Block S M 1998
30 Force and Velocity Measured for Single Molecules of RNA Polymerase
31 *Science* **282** 902-7
- 32
33 [19] Forde N R, Izhaky D, Woodcock G R, Wuite G J L and Bustamante C 2002
34 Using mechanical force to probe the mechanism of pausing and arrest during
35 continuous elongation by Escherichia coli RNA polymerase *PNAS* **99** 11682-7
- 36
37 [20] Abbondanzieri E A, Greenleaf W J, Shaevitz J W, Landick R and Block S M
38 2005 Direct observation of base-pair stepping by RNA polymerase *Nature* **438**
39 460-5
- 40
41 [21] Tang G Q, Roy R, Bandwar R P, Ha T and Patel S S 2009 Real-time
42 observation of the transition from transcription initiation to elongation of the
43 RNA polymerase *Proc Natl Acad Sci U S A* **106** 22175-80
- 44
45 [22] Skinner G M, Baumann C G, Quinn D M, Molloy J E and Hoggett J G 2004
46 Promoter Binding, Initiation, and Elongation By Bacteriophage T7 RNA
47 Polymerase *The journal of Biological Chemistry* **279** 3239-44
- 48
49 [23] Saecker R M, Record Jr M T and deHaseth P L 2011 Mechanism of Bacterial
50 Transcription Initiation: RNA Polymerase - Promoter Binding, Isomerization
51 to Initiation-Competent Open Complexes, and Initiation of RNA Synthesis
52 *Journal of Molecular Biology* **412** 754-71
- 53
54 [24] Levens D, Baranello L and Kouzine F 2016 Controlling gene expression by
55 DNA mechanics: emerging insights and challenges *Biophys Rev* **8** S23-S32
- 56
57 [25] Gore J, Bryant Z, Stone M D, Nollmann M, Cozzarelli N R and Bustamante C
58 2006 Mechanochemical analysis of DNA gyrase using rotor bead tracking
59 *Nature* 100-4
- 60 [26] Brown P O and Cozzarelli N R 1979 A sign inversion mechanism for

- enzymatic supercoiling of DNA *Science* **206** 1081-3
- [27] Cheng B, Zhu C-X, Ji C, Ahumada A and Tse-Dinh Y-C 2003 Direct interaction between Escherichia coli RNA polymerase and the zinc ribbon domains of DNA topoisomerase I *Journal of Biological Chemistry* **278** 30705-10
- [28] Zechiedrich E L, Khodursky A B, Bachellier S, Schneider R, Chen D, Lilley D M and Cozzarelli N R 2000 Roles of topoisomerases in maintaining steady-state DNA supercoiling in Escherichia coli *J Biol Chem* **275** 8103-13
- [29] Thomen P, Lopez P J and Heslot F 2005 Unravelling the Mechanism of RNA-Polymerase Forward Motion by Using Mechanical Force *Physical Review Letters* **94** 128102
- [30] Ma J, Bai L and Wang M D 2013 Transcription under Torsion *Science* **340** 1580-3
- [31] Czyz A, Mooney R A, Iaconi A and Landick R 2014 Mycobacterial RNA Polymerase Requires a U-Tract at Intrinsic Terminators and Is Aided by NusG at Suboptimal Terminators *Mbio.* **5** e00931
- [32] Reznikoff W and Gold L 2014 *Maximizing gene expression* vol 9: Elsevier
- [33] Kim P and Lee C H 2014 Fast probability generating function method for stochastic chemical reaction networks *MATCH Commun. Math. Comput. Chem* **71** 57-69
- [34] Thattai M and Van Oudenaarden A 2001 Intrinsic noise in gene regulatory networks *Proceedings of the National Academy of Sciences* **98** 8614-9
- [35] Howard J 2001 *Mechanics of motor proteins and the cytoskeleton*
- [36] Zhou Y and Martin C T 2006 Observed Instability of T7 RNA Polymerase Elongation Complexes Can Be Dominated by Collision-induced "Bumping"* *THE JOURNAL OF BIOLOGICAL CHEMISTRY* **281** 24441-8
- [37] Epshtein V and Nudler E 2003 Cooperation Between RNA Polymerase Molecules in Transcription Elongation *Science* **300** 801-5
- [38] Herbert K M, Greenleaf W J and Block S M 2008 Single-Molecule Studies of RNA Polymerase: Motoring Along *Annu. Rev. Biochem* **77** 149-76
- [39] Battaile C C 2008 The Kinetic Monte Carlo method: Foundation, implementation, and application *Comput. Methods Appl. Mech Engrg.* **197** 3386-98
- [40] Lesne A, Victor J-M, Bertrand E, Basyuk E and Barbi M 2018 *Molecular Motors*: Springer, Chapter 11, pp 215-32
- [41] Tantale K, Mueller F, Kozulicpirher A, Lesne A, Victor J M, Robert M, Capozzi S, Chouaib R, Bäcker V and Mateoslangerak J 2016 A single-molecule view of transcription reveals convoys of RNA polymerases and multi-scale bursting *Nature Communications* **7** 12248
- [42] Sanchez A and Golding I 2013 Genetic Determinants and Cellular Constraints in Noisy Gene Expression *Science* **342** 1188-93